AD_____

Award Number: W81XWH-12-1-0093

TITLE: Novel Approaches to Breast Cancer Prevention and Inhibition of Metastases

PRINCIPAL INVESTIGATOR: Prof. Dr. Josef Penninger

CONTRACTING ORGANIZATION: IMBA – Institut fuer Molekulare Biotechnologie GmbH
Vienna, 1030 AT

REPORT DATE: October 2014

TYPE OF REPORT: Annual Report

PREPARED FOR: U.S. Army Medical Research and Materiel Command
Fort Detrick, Maryland 21702-5012

DISTRIBUTION STATEMENT: Approved for Public Release;
Distribution Unlimited

REPORT DOCUMENTATION PAGE

Form Approved
OMB No. 0704-0188

1. REPORT DATE	**2. REPORT TYPE**	**3. DATES COVERED**
October 2014	Annual	30 Sep 2013 – 29 Sep 2014

4. TITLE AND SUBTITLE

Novel Approaches to Breast Cancer Prevention and Inhibition of Metastases

5a. CONTRACT NUMBER

5b. GRANT NUMBER
W81XWH-12-1-0093

5c. PROGRAM ELEMENT NUMBER

6. AUTHOR(S)

Prof. Dr. Josef Penninger

E-Mail: Josef.Penninger@imba.oeaw.ac.at

5d. PROJECT NUMBER

5e. TASK NUMBER

5f. WORK UNIT NUMBER

7. PERFORMING ORGANIZATION NAME(S) AND ADDRESS(ES)

IMBA – Institut fuer Molekulare Biotechnologie GmbH
Dr. Bohrgasse 3
Wien 1030
Austria

8. PERFORMING ORGANIZATION REPORT

9. SPONSORING / MONITORING AGENCY NAME(S) AND ADDRESS(ES)
U.S. Army Medical Research and Materiel Command
Fort Detrick, Maryland 21702-5012

10. SPONSOR/MONITOR'S ACRONYM(S)

11. SPONSOR/MONITOR'S REPORT NUMBER(S)

12. DISTRIBUTION / AVAILABILITY STATEMENT
Approved for Public Release; Distribution Unlimited

13. SUPPLEMENTARY NOTES

14. ABSTRACT

We combine fly genetics with haploid ES cell mutagenesis and *in vivo* mouse genetics to functionally characterize candidate breast cancer genes. Using mouse genetics we have progressed in defining the role of RANKL/RANK in sex hormone-driven breast cancer. Moreover, we have now provided strong evidence that inactivation of RANK also markedly delays and in some cases even prevents the development of BRCA1-mutant breast cancer. If correct this could lead to first cancer prevention trials in BRCA1 carriers using RANKL blockade. Using *Drosophila* modeling of Ras-driven transformation, we performed a near-genome wide screen for genes that control tumor progression. Using this system we have functionally identified multiple novel cancer genes that also play a role in breast cancer, e.g. the surface receptor TSPAN6. TPAN6 expression also correlates with prognosis in human breast cancer patients. Finally, we have progressed in generating a haploid ES cell library for all researchers and have already generated more than 46000 murine ES cell clones targeting ~ 11500 different genes. These can now been used to perform synthetic lethal drug screens or to uncover resistance to defined drugs. Thus, we continue on all proposed aims with the vision to provide rapid functional annotation of breast cancer genes and, in case or RANKL/RANK, to provide the experimental underpinning for clinical prevention trials with the vision to one day be able to prevent breast cancer.

15. SUBJECT TERMS

Genome wide functional genetics, haploid stem cells, *Drosophila* cancer modeling, breast cancer prevention, BRCA1 carriers

16. SECURITY CLASSIFICATION OF:			17. LIMITATION OF ABSTRACT	18. NUMBER OF PAGES	19a. NAME OF RESPONSIBLE PERSON
					USAMRMC
a. REPORT	b. ABSTRACT	c. THIS PAGE			19b. TELEPHONE NUMBER *(include area code)*
U	U	U	UU	24	

Table of Contents

Page

INTRODUCTION:

Multiple genes and pathways have been identified that might have a role in breast cancer. One challenge is to elucidate the function of these molecular pathways and to understand their link to the initiation and progression of breast cancer. Moreover, for the patients it is key to attempt to translate such fundamental findings into possibly future therapies. In my grant proposal, I therefore proposed to integrate cancer modeling in Drosophila melanogaster, murine haploid ES cell technologies and in vivo functional mouse genetics to discover and validate novel genes with direct relevance to breast cancer. In addition, I proposed a project that due to an already approved drug could have a rapid impact on prevention and treatment of breast cancer, i.e. to explore the role of RANKL/RANK in breast cancer.

BODY:

The following three tasks were proposed

1. **Dissecting the role of RANKL/RANK in mammary cancer.**
2. **Functional validation of breast cancer genes using *Drosophila* genetics.**
3. **Modelling breast cancer and cancer metastases using haploid ES cell technology.**

1. Dissecting the role of RANKL/RANK in mammary cancer.

Background: My group generated the first RANKL mutant mice, providing definitive proof that RANKL (OPGL, TRANCE, or ODF) is the master regulator of bone loss[1,2], thus opening new possibilities to develop the first rationale therapies against bone loss in multiple diseases such as osteoporosis, leukemia, AIDS, arthritis, and, importantly, cancer related skeletal events. During the course of our studies, we identified another essential function for RANKL/RANK: this system is essential for the formation of a lactating mammary gland in pregnancy and that RANKL expression is induced by the female sex hormone progesterone[3], thus providing a molecular and evolutionary explanation for gender bias and the high incidence of osteoporosis in females. We have also shown that RANKL and RANK are expressed in primary breast cancers and breast cancer-derived cell lines and that the RANKL/RANK system can function as a soil factor that controls bone metastases[4], a finding that provided, among work from other groups[5,6], a mechanistic underpinning for clinical trials to delay bone metastases in prostate and breast cancer. In prostate cancer, blocking RANKL can indeed delay the first occurrence of bone metastases[7]. The already FDA approved RANKL blocking antibody (Denosumab) is currently being tested in clinical trials preventing metastases in breast cancer patients. Moreover, it has been shown that blocking the RANKL/RANK pathway can indeed increase survival in a mouse model of breast cancer bone metastasis[8].

The Women's Health Initiative and the Million Women Study have shown that hormone replacement therapy (HRT) is associated with an increased risk of incident and fatal breast

cancer[9,10]. In particular, synthetic progesterones (progestins) used in HRT and contraceptives increase the risk of being diagnosed with breast cancer. Based on the clinical importance of RANKL inhibition already being approved for bone loss[11,12] and the essential physiological function of RANKL/RANK in mammary epithelial proliferation in pregnancy in response to sex hormones[3,13], we initially came up with the idea that RANKL/RANK might play a role in breast cancer initiation. My group[14] and Gonzalez-Suarez *et al*.[5] were indeed able to show that the RANKL-RANK system is a key regulator of hormone (progestin)- and oncogene (Neu)-driven mammary cancer. Mechanistically, RANKL promotes the proliferation of mammary epithelial cells, rescues mammary epithelium from death after DNA damage, and regulates renewal of breast cancer stem cells[14]. Therapeutic inhibition of RANKL reduced the incidence of hormone driven breast cancer from 100 to ~ 10% in a mouse model[5]. Thus, 10 years after we proposed that RANKL/RANK might have a role in breast cancer[3], our data and parallel work by the group of Bill Dougell[5] definitively showed that RANKL/RANK can link sex hormones to the development of breast cancer.

Results: In my first year report I highlighted our work on work on downstream activation pathways for RANKL/RANK in breast cancer; to this end we deleted the key signaling molecules TRAF6 and NFATc1 in mammary epithelial cells using K5Cre and MMTV-Cre mice. We also deleted RANK using K5Cre as delete strain, which resulted in a complete block in the formation of a lactating mammary gland. The conclusions of these experiments were that deletion of RANK using K5-Cre markedly delays the development of hormone-driven mammary cancer and that TRAF6, but not NFATc1, appear to mediate these effects. We also showed using RANKLfloxed mice[15] that RANKL appears to function in mammary epithelial cells rather than in regulatory T cells, as proposed by others[6]. Moreover, we assayed sera from premenopausal women at high risk of developing breast cancer due to *BRCA1* mutations. Our first data showed that women with *BRCA1* mutations exhibit deregulated RANKL and reduced OPG (the natural inhibitor of RANKL) levels during their menstrual cycle, resulting in an increased exposure to RANKL. Thus, the RANKL/RANK/OPG system appears to be deregulated in females with increased risk of breast cancer and with diagnosed breast cancer; these data now needs to be expanded to larger cohorts.

Since we found a deregulation of RANKL/OPG serum levels in BRCA1 mutation carriers and such carriers are at very high risk to develop breast cancer, we have now made considerably efforts to investigate the role of RANKL/RANK in *BRCA1*-mutant breast cancer. Tumors from *BRCA1* mutation carriers are in general triple negative "basal" phenotype and thus have a bad prognosis and limited treatment options. Interestingly, RANK is expressed exactly in such "basal" mammary epithelial cells, probably controlling expansion of epithelial progenitor populations. We therefore deleted RANK in the mammary epithelium using a mouse model of *BRCA1/p53* double mutation-driven breast cancer[16]. Of note, in this mouse model blocking of progesterone receptors results in delayed mammary tumor formation[16]. To perform these experiments we had to introduce 4 different mutant alleles into one mouse background, a tour-de-force of mouse breeding (Figure 1, left panel). Finally we derived such mice used WapCre. Importantly, our results indicate that loss of RANK in mammary epithelial cells that carry *p53* and *BRCA1* mutations, significantly alters the onset of mammary cancer and ~ 25% of the mice

remained entirely tumor free (Figure 1, right panel). Of note, RANK is highly expressed in the mammary tumors due to *BRCA1-p53* mutations and this expression is abrogated in our WapCre RANK mutants confirming that our experimental deletion strategy has indeed worked (Figure. 2).

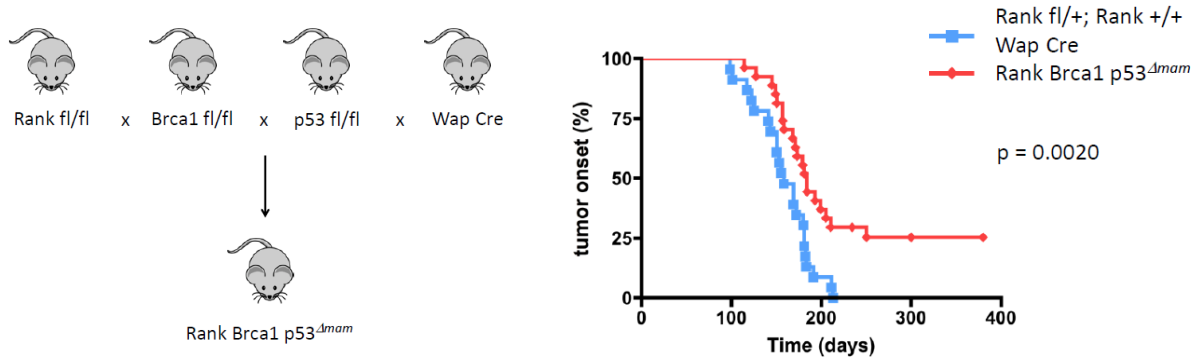

Figure 1. Breeding scheme (left panel) and onset of palpable mammary tumors in nulliparous female littermate mice that are mutant for *BRCA1* and *p53* and carry either both (Rank+/+) or one allele of RANK (Rank fl/+) (both used as controls, blue line) or are mutant for RANK (red line). For deletion of RANK we used the Wap-Cre line. The P value between the RANK expressing control and *Rank* mutant cohorts is indicated. Of note, we did not find any differences when we compared mice that are wild type or heterozygous for *Rank* (not shown).

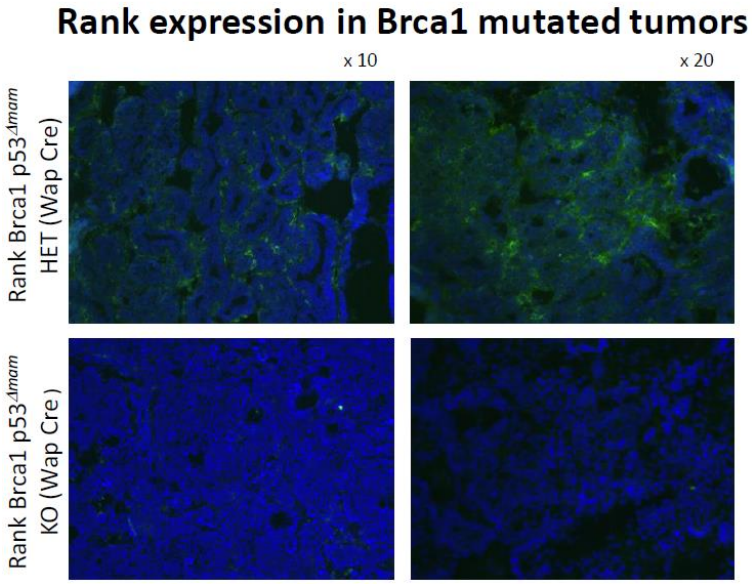

Figure 2. Immunohistochemistry to detect RANK in mammary tumors driven by WapCre-mediated deletion of *BRCA1* and *p53*. Note absence of RANK immunostaining in tumors from mice that carry a *Rank* deletion.

Since WapCre is highly induced during pregnancy, though it is also constitutively active in epithelial cells from nulliparous females, we speculated that the one might get even stronger effects when Rank is mutated using K5Cre. We therefore generated K5-Cre BRCA1/*p53* mutant mice that do not or still express RANK in the mammary epithelium (Figure 3, left panel, shows the breeding scheme). Intriguingly, our first results indicate that K5-Cre mediated loss of RANK in mammary epithelial cells completely prevents the onset of mammary epithelial hyperproliferation in mice that carry *p53* and *BRCA1* double mutations. However, as a word of caution, these data are from ~ 4 month old females and we could not study older females because these mutant mice also develop skin cancer which pre-empted long term follow-up studies; thus we cannot exclude that mammary tumors might develop at later stages. To get "around this", we have now initiated experiments transplanting mammary tissue from K5-Cre *BRCA1/p53* mutant mice in the presence of absence of RANK into immunodeficient RAG mutant host females. These data using two different Cre delete lines indicate that deletion of RANK delays, and in some cases even prevents, the occurrence of *BRCA1/p53* mutant mammary tumors.

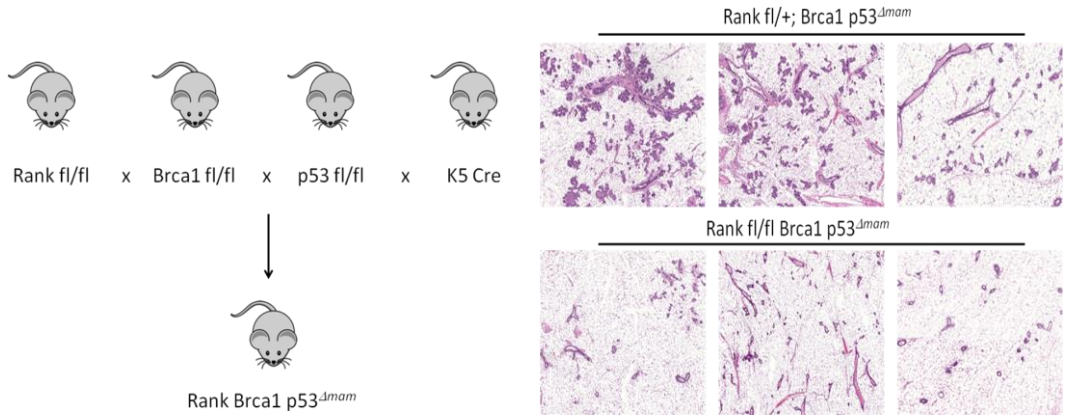

Figure 3. Breeding scheme (left panel) and H&E analyses (right panels) of mammary tissue of three different nulliparous littermate mice that are mutant for *BRCA1* and *p53* and carry either one allele of *Rank* (Rank fl/+) or are mutant for *Rank* (Rank fl/fl). Note epithelial hyperproliferation in the RANK expressing "control" females.

How does deletion of RANK delay and even sometimes prevent the development of mammary tumors in *BRCA1/p53* mutant mice? To address this issues we assayed expansion of mammary progenitor cells in response to steroid hormones. Interestingly, sex hormone-induced expansion of mammary stem cells is markedly impaired in our *Rank/BRCA1/p53* triple KO mice as compared to control wild type mice and *Brca1/p53* double mutant mice (Figure 4). Of note, this hormone-induced mammary stem cell expansion is impaired in both WapCre *Rank/BRCA1/p53* triple KO mice and K5Cre *Rank/BRCA1/p53* triple KO mice (not shown). Moreover, purified basal epithelial cell from *Rank/BRCA1/p53* triple KO mice form significantly less colonies in matrigel assays (Figure 5, left panel) and triple mutant mice display a decreased number of $BrdU^+$ cells/duct 2 hours after BrdU injection compared to *BRCA1/p53* double KO mice (Figure 5, right panel).

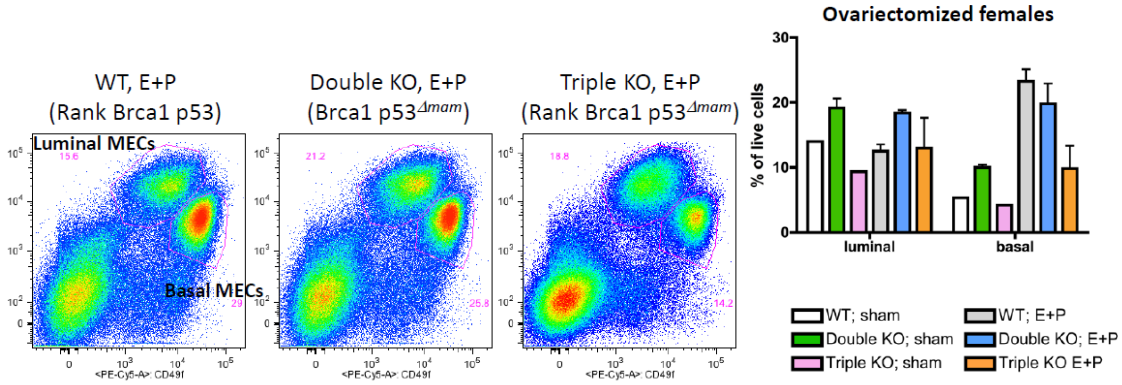

Figure 4. Representative FACS blots (left panels) and quantification (right panel) of luminal and basal mammary epithelial cells (based on $CD24^{+}CD49f^{high}$ immunostaining) in ovariectomized wild type (WT), *BRCA1/p53* double mutant, and *Rank/BRCA1/p53* triple knock-out mice left untreated (sham) or treated with estrogen + progesterone (E + P).

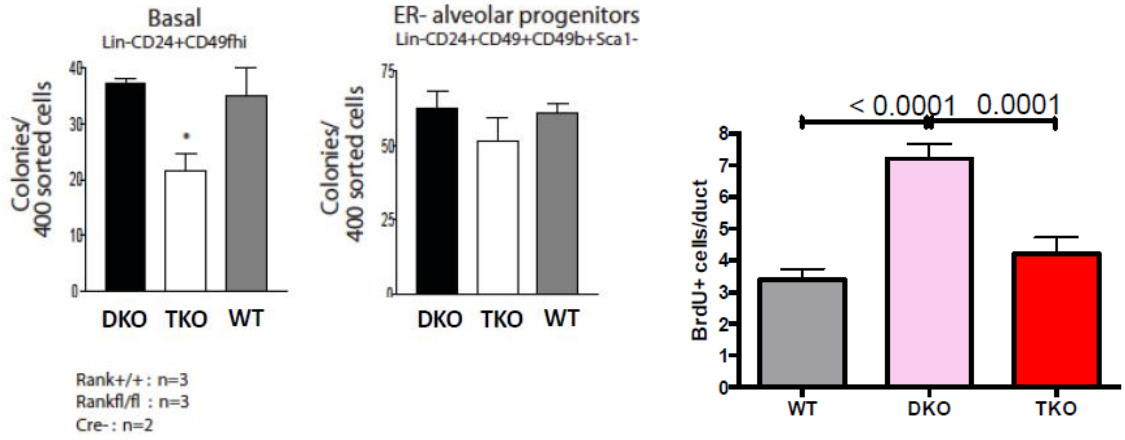

Figure 5. Left panels. Colony formation of basal and alveolar progenitors isolated from wild type (WT), *BRCA1/p53* double (DKO), and *Rank/BRCA1/p53* triple (TKO) knock-out mice using matrigel assays. **Right panel:** $BrdU^{+}$ cells/duct in wild type (WT), *BRCA1/p53* double (DKO), and *Rank/BRCA1/p53* triple (TKO) knock-out mice.

Taken together these data indicate that deletion of RANK markedly slows the development *BRCA1/p53* mutant mammary cancer, probably due to an effect on the expansion of basal mammary progenitor cells. These results also provide a rationale to possibly initiate phase II/III breast cancer prevention trials in humans BRCA1 carriers using the already FDA-approved anti-RANKL antibody.

2. Identification of cancer genes using *Drosophila* genetics.

Background: Many developmental pathways and signaling cascades implicated in cancer have been originally identified in *Drosophila melanogaster*[17-19] and oncogenic signaling pathways such as Ras and Notch are conserved from fly to human[20]. Moreover, epithelial tumor cell metastasis has been modeled in fly larvae[21,22]. Thus, fundamental mechanisms of oncogenic transformation and metastases are highly conserved among flies and humans. Researchers at our campus have created the now largest global RNA interference library in the world representative of nearly all expressed (~ 14,500) *Drosophila* genes; thus we have local access to a library of *Drosophila* where every fly gene can be inactivated via RNAi *in vivo* using tissue specific promoters[23]. We are therefore in a unique position to examine the role of genes in cancer cell growth, invasion, and metastasis in a whole organism and near genome-wide levels.

Results: We have successfully modeled hyperplasia in larval epithelial cells using activated Ras^{V12} which allowed us to identify hundreds of novel genes that modulate Ras-induced transformation (Figure 6). Expression of the human orthologs of our primary fly hits were significantly ($p < 0.00002$) downregulated in thousands of human tumors making fly a viable model system to study human cancer (Figure 7). In secondary fly screens we could confirm more than 80% of these hits using different hairpins and different read-outs (not shown). Thus, our functional screen to identify conserved genes that control growth of dRasV12 expressing epithelial tumors has identified many known mammalian cancer and metastasis genes. Importantly, we also identified multiple novel candidate tumor suppressors.

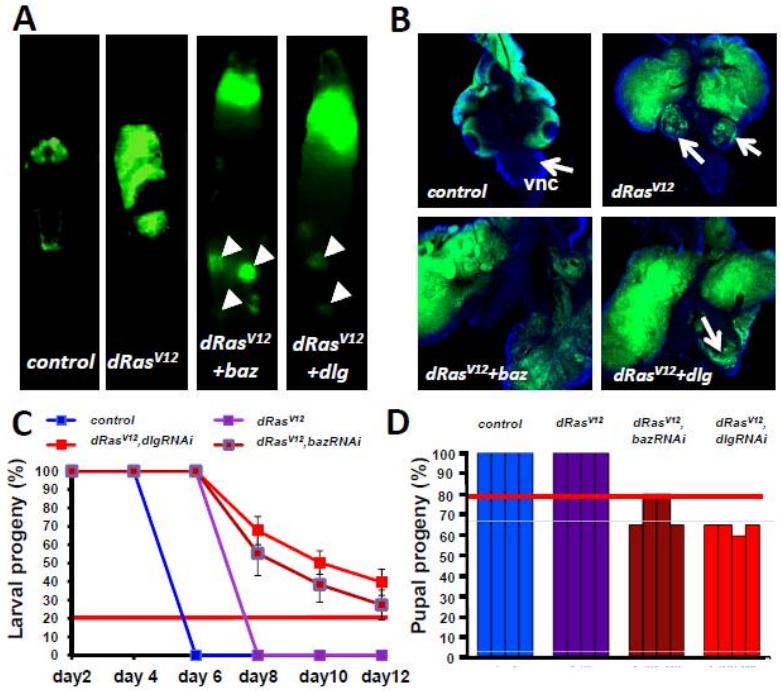

Figure 6. A) GFP-labeled epithelial eye disc cells in control, *UAS-dRasV12, UAS-dRasV12;UAS-IR baz*, and *UAS-dRasV12;UAS-IR dlg* expressing flies. Note tumor growth in *UAS-dRasV12* lines and formation of metastaic foci (arrows) in flies co-expressing dRasV12 and baz or dlg. Images are from day 8 after egg laying (AEL). Magnifications X 8. B) Dissected cephalic complexes from control and dRasV12

transformed eye discs at d5 AEL (top panels). Lower panels show invasive tumor formation upon co-expression of *UAS-IR baz* or *UAS-IR dlg* in the eye disc epithelium of fly larvae at d8 AEL. Magnifications X 25 (top) and X 40 (bottom panel). Arrows indicate brain lobes. Note fusion of brain lobes with eye discs upon invasive tumor formation in the lower right panel. C) Quantification of larval arrest (% larval progeny at the indicated days AEL) and D) pupal progeny in control, *UAS-dRasV12, UAS-dRasV12; UAS-IR baz* and *UAS-dRasV12; UAS-IR dlg* flies. In D individual experiments are shown for day 8 AEL. Red lines in C and D indicate the cut-off (Z-score 1.65) at which we always observed a phenotype in the positive control *UAS-dRasV12; UAS-IR baz* and *UAS-dRasV12; UAS-IR dlg* lines.

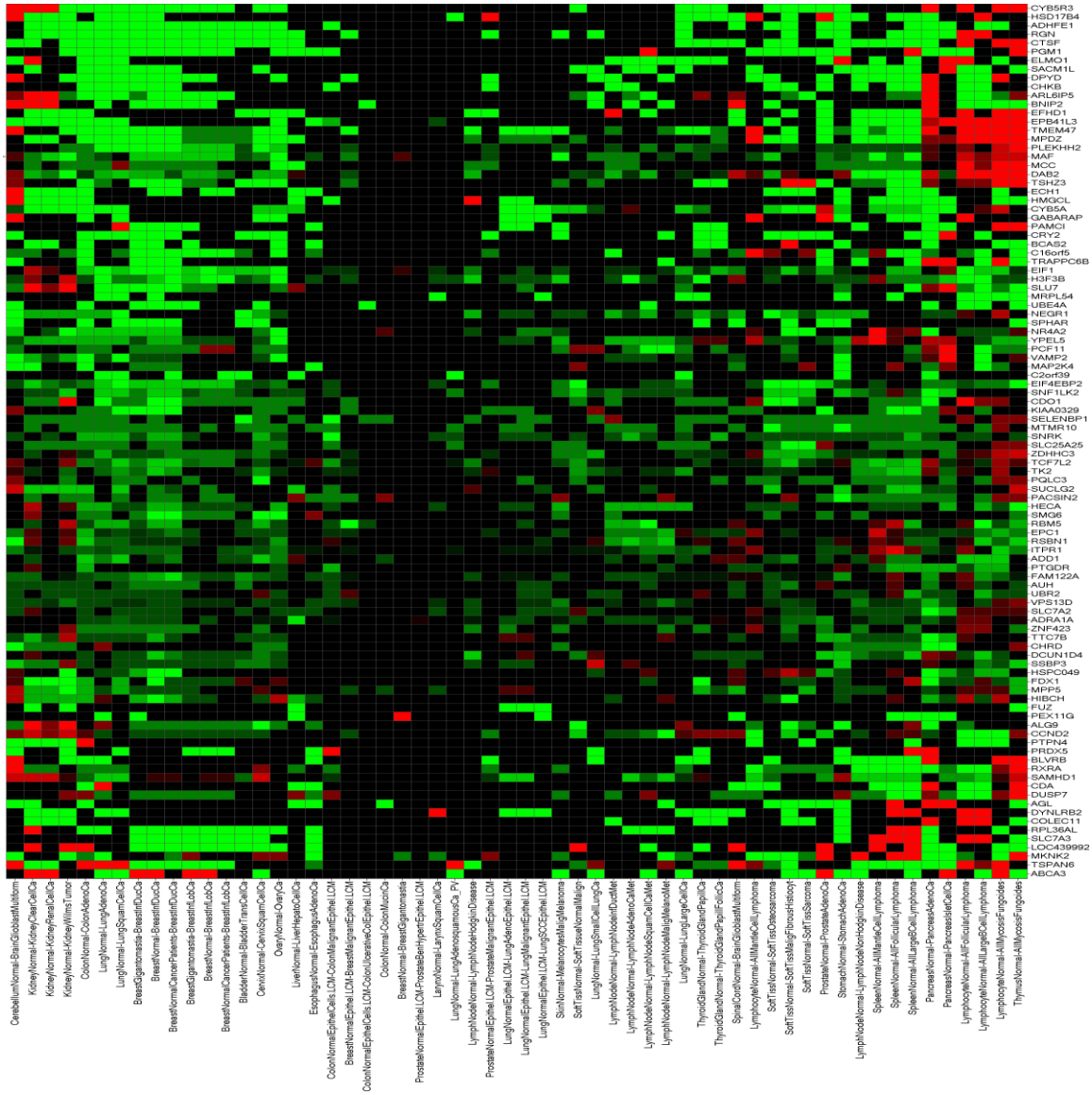

Figure 7. Heatmap of the differential expression score of the top 100 human ortholog candidate tumor suppressors tested for differential expression between a cancer sample set and its corresponding normal tissue. The gene symbol (Y axis) and the respective comparisons (X-axis) are listed. Increased expression in tumor as compared to the corresponding normal tissue is shown in red, reduced expression in tumors is shown in green. Black boxes indicate no changes.

One of the most significant categories that appeared in all gene network analyses (KEEG and C2 pathways) performed on our hits was cell adhesion. Moreover, we had generated a list of primary *Drosophila* hits that showed brain invasion and formation of distinct "metastatic" foci. We therefore focused our attention on novel candidate genes with a predicted role in cell adhesion and which showed an invasive phenotype in our assay. Besides our positive controls *baz* and *dlg*, there were only two additional candidate genes that fulfilled these requirements: Lachesin, an IgLON-family molecule implicated in septate junctions and epithelial integrity. LSAMP, the mammalian Lachesin ortholog, has been implicated as candidate tumor suppressor in renal cell carcinomas and osteosarcoma[24]. The second candidate gene was *Tsp29fb*, coding for a member of the tetraspanin family of membrane-spanning proteins. *Drosophila* Tsp29fb mRNA expression is found in various larval tissues reaching the highest level at the third instar larval stage and in adults (http://flybase.org/reports/FBgn0032075.html). RNAi mediated tsp29Fb depletion in untransformed eye-antenna discs had no overt effect on eye development (Figure 8A). However, on a *dRasV12* background RNAi mediated knock-down of Tsp29Fb resulted in larval arrest and local invasion of GFP-labeled tumor cells into the ventral nerve cord (Figure 8A). Importantly, mechanistically, Tsp29Fb appears to cooperate with EGFRs in *Drosophila* (not shown). The function of the mammalian Tsp29fb ortholog TSPAN6 (*TM4SF6*) was entirely unknown. We therefore set out to characterize the role of TSPAN6 in cancer.

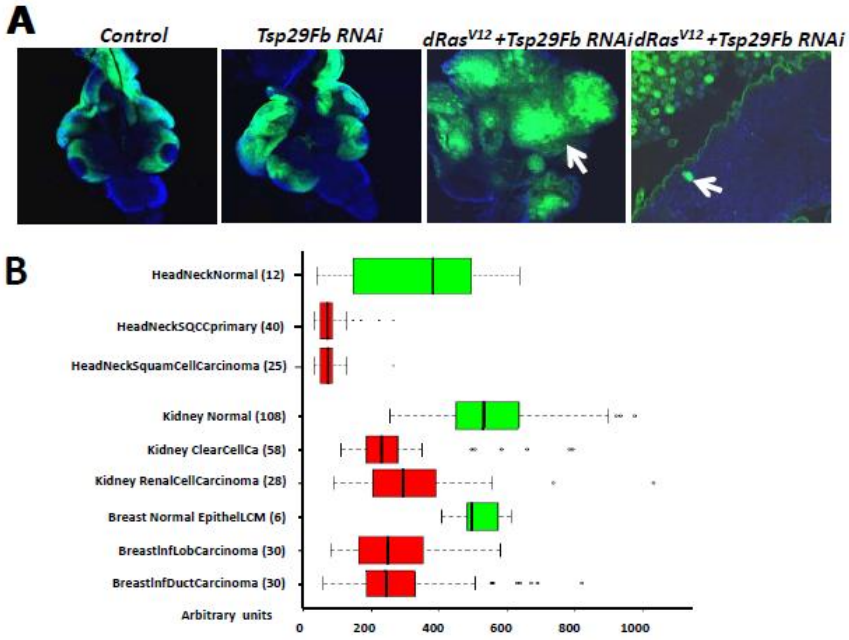

Figure 8. A) Tsp29Fb RNAi knockdown in developing third instar larval eye discs does not result in an overt phenotype when compared to normal control discs. Images are from d6 AEL. Co-expression of tsp29Fb RNAi with dRasV12 results in neoplastic transformation of eye-antenna discs and epithelial overgrowth in developing third instar larvae (d8AEL) and infiltration of GFP-labeled cells (arrow) into the ventral nerve cord (right panel). All magnifications X 25; right panel magnification X 40. B) Box plots showing relative TSPAN6 mRNA expression in the indicated human tumors and matched normal tissue. Microarray data were obtained by using two different TSPAN6 probes. Numbers of samples for each tumor and matched tissues are shown in brackets. LCM, laser capture microscopy obtained samples.

In humans, TSPAN6 mRNA is expressed in multiple tissues including kidney, liver, thyroid, prostate, pancreas, uterus, testis, salivary and adrenal glands, or smooth and cardiac muscle; TSPAN6 mRNA was below detection in bone marrow or peripheral blood cells. Immunostaining showed that human and mouse TSPAN6 protein is primarily expressed in epithelial cells. To determine if TSPAN6 has a potential role in human tumorigenesis, we assessed mRNA expression in multiple paired tumors and organ-matched normal tissue samples from cancer patients. Intriguingly, *TSPAN6* mRNA expression was markedly decreased in a plethora of primary human tumors such as pancreas carcinomas, squamous head and neck cancer, ovarian cancers, kidney, and, importantly breast cancer (Figure 8B). SNP chip analysis of human tumor cell lines revealed that the *TSPAN6* locus in the Xq22.1 genomic region is frequently deleted in breast cancer cells: 24/59 cell lines analyzed showed chromosomal deletions encompassing the *TSPAN6* locus (Figure 9, left panel, and not shown). Of note, in these breast cancer cell lines, the TSPAN6 region is more frequently deleted than the E-cadherin (*cdh1*) locus. We also observed deletions spanning the TSPAN6 locus in primary breast cancer. Importantly, typical for tumor suppressors, we detected defined focal deletions and break-points at the genomic region containing the *TSPAN6* locus in primary human breast tumors (Figure 9, right panel). Thus, TSPAN6 is commonly down-regulated in multiple human breast cancers and the genomic region encompassing the *TSPAN6* locus is frequently deleted in breast tumor cell lines and primary human breast cancer.

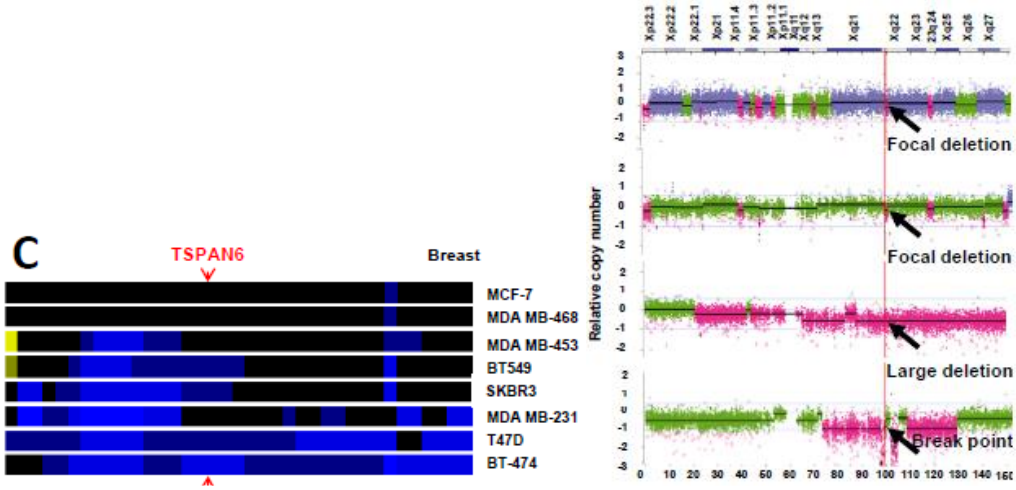

Figure 9. Left panel: SNP maps of the X chromosomal region p22.3-q27 showing deletions of the TSPAN6 locus (red arrow) in human breast and kidney cancer cell lines. Light blue indicates a copy number decrease; dark blue indicates a loss of the indicated regions; shades of yellow indicate increased copy numbers; black indicates normal diploid DNA content. For the presented copy number analysis, 50 and 100k Affymetrix SNP chips were used. Right panel: SNP maps showing focal deletions and chromosomal breakpoints at the TSPAN6 locus in 4 different primary human breast cancer samples. Vertical red line marks chromosomal position of the TSPAN6 locus; blue indicates amplifications; magenta-deletions; and green normal copy number of the indicated regions of the X-chromosome. Chromosomal position is indicated on the X axis in megabases. Copy numbers are shown on the logarithmic Y axis (Copy number = 2*2^y). For the presented copy number analysis, SNP 6.0 (1.8 million) chips were used.

Our data show that TSPAN6 expression is reduced in multiple human tumors and that genomic *TSPAN6* deletions are frequently found in tumor cell lines and also in primary breast cancer. We therefore explored the possibility whether TSPAN6 levels might correlate with prognosis in breast cancer patients. Since the biological mechanisms of tumor development and progression in breast cancer differ according to their molecular phenotype[25], we evaluated TSPAN6 mRNA expression in three major molecular subtypes of breast cancer, i.e. ER-HER2- ("basal-like"), ER-HER2+ ("HER2-overexpressing"), and ER+HER2- ("luminal") subtypes. Intriguingly, whereas TSPAN6 mRNA levels were not prognostic in patients with ER-HER2- and ER-HER2+ tumors (not shown), we observed a significant association of TSPAN6 expression with metastases-free survival in patients diagnosed with ER+HER2- breast cancer. Specifically, low TSPAN6 mRNA expression correlated with a poor prognosis in multiple independent breast cancer patient cohorts[26-28] (Figure 10A).

Since this correlation was found in patients diagnosed with ER+ breast tumors, we next assessed patients that had received tamoxifen adjuvant monotherapy as all patients with ER+ tumors receive hormonal anti-cancer therapy today. In these tamoxifen-treated patients, we observed that TSPAN6 mRNA levels at the time of diagnosis predicted long term disease outcome, i.e. patients carrying TSPAN6low breast tumors showed a significantly worse survival than patients with TSPAN6high breast cancer (Figure 10B). Low TSPAN6 expression levels were significantly associated with high histologic grade (poorer differentiation) of the breast tumor ($p=1.3$ E-4) and the presence of positive lymph nodes ($p=0.04$) but not with tumor size or age of the patient. A multivariate Cox regression analysis showed that TSPAN6 expression levels had prognostic value independent of previously established prognostic factors in ER+ breast breast cancer such as lymph node status or tumor histological grade (Figure 10C). Thus, among patients with ER+ breast tumors, TSPAN6low mRNA expression is associated with advanced tumor grades, poorer survival, and enhanced risk of distant metastases. Finally, we tested whether TSPAN6 mRNA expression might also correlate with survival in patients diagnosed with low clinical risk ER+ tumors as defined by their molecular subtype (also known as "luminal A" tumors). Intriguingly, our data for this cohort show that TSPAN6low expression predicts poor clinical outcome even in luminal A patients with lymph node negative disease (Figure 10D,E). Thus, TSPAN6 appears to be a novel prognostic biomarker for ER+ breast cancer and TSPAN6high expression defines a subpopulation of ER+ breast cancer patients with very good clinical prognosis.

We finally generated *TSPAN6* whole body knock-out mice as well as *TSPAN6*^{floxed} mice which were crossed to K5Cre deleter lines to delete TSPAN6 in the mammary epithelium. These mice are viable and have no overt macroscopic phenotype. The whol-body and epithelial-specific *TSPAN6* mutant females were the challenged with MPA and DMBA to induce hormone-driven mammary tumors. Importantly, when we challenged whole body mice *TSPAN6* mutant with MPA plus DMBA to drive breast cancer, we observed markedly enhanced onset of first palpable tumors and secondly reduced overall survival of the mice (Figure 11). Similar to the whole body mutant mice, deletion of TSPAN6 in the mammary epithelium markedly enhanced mammary tumor onset and significantly reduced the survival of the female mice (Figure 12). Thus, TSPAN6 appears to function as a novel tumor suppressor for breast cancer.

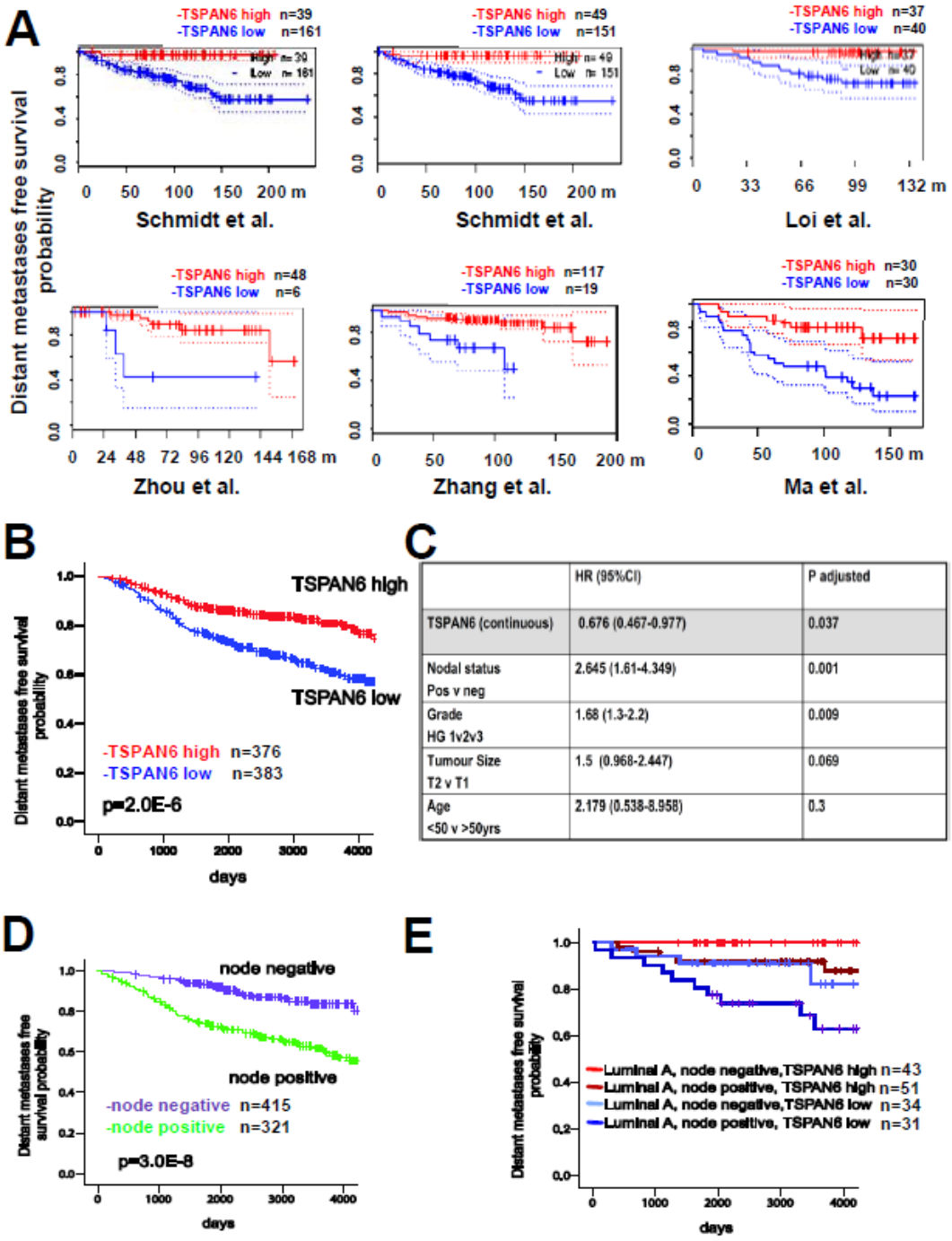

Figure 10. A) Kaplan-Meier curves from independent studies showing distant metastases-free survival relative to TSPAN6 mRNA expression in patients diagnosed with estrogen receptor (ER) positive breast cancer. Data are from studies by Schmidt et al, Loi et al, Zhang et al, Zhou et al, and Ma et al, (http://gibk21.bse.kyutech.ac.jp/PrognoScan/index.html). Dashed lines indicate the 95% confidence interval. n = number of patients assigned to the TSPAN6high (red) and TSPAN6low (blue) cohorts. X axis shows time after diagnosis in months (m). In all cases $p<0.05$ (log-rank test, minimal corrected p value (Pcor=4φ(z)/(z)+ φ(z){z-1(1/z)}log{1-ε)2/ε2). B) Kaplan-Meier curve for ER+ patients treated with

tamoxifen adjuvant monotherapy stratified by TSPAN6 high vs. low expression divided at the median (see experimental procedures). Endpoint is first distant metastatic event. p<0.000002 (log-rank test). C) Multivariate Cox regression analysis for TSPAN6 levels, nodal status, tumor grade, tumor size, and age in patients with ER+ breast cancer. Hazard ratios (HR), 95% confidence intervals (95% CI) and p-values are shown. TSPAN6 is treated as a continuous variable and hence cut-off independent, high-lighting the independent prognostic marker value of TSPAN6 mRNA expression in ER+ tamoxifen treated patients. Analysis was performed on 382 patients with confirmed ER+/HER2- status by gene expression with all variables available. D) Kaplan Meier graphs showing cumulative survival in lymph node negative versus lymph node positive ER+ breast cancer patients demonstrating the importance of nodal disease as a prognostic factor in breast cancer. E) Kaplan- Meier graph showing cumulative survival of patients diagnosed with Luminal A breast cancer based on TSPAN6 mRNA expression levels and the lymph node status. TSPAN6high expression in Luminal A tumors with and without lymph node invasion defines a group of patients with a very good prognosis. Patients were assigned to TSPAN6high or TSPAN6low groups using median cutoff. In all cases p<0.05 (log-rank test).

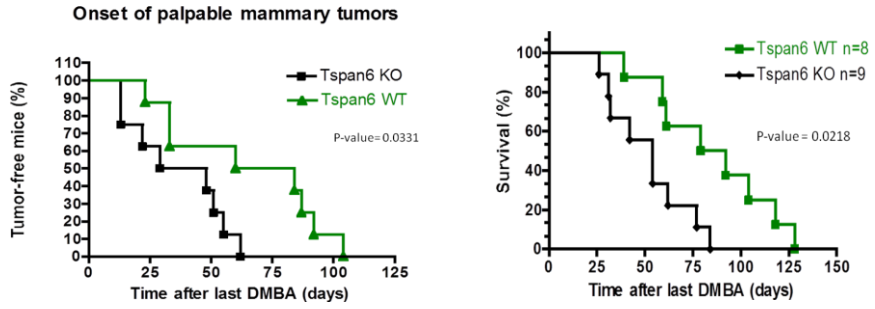

Figure 11. Onset of palpable mammary tumors (left panel) and overall survival (right panel) in TSPAN6 expressing and TSPAN6 mutant age-matched littermate control females treated with the progestin MPA and the carcinogen DMBA. For MPA/DMBA carcinogenesis, nulliparous, six-week old female mice were s.c. implanted with MPA pellets and treated orally with DMBA as indicated for 8 week. Data are shown as percentage of tumor free mice after the last DMBA challenge.

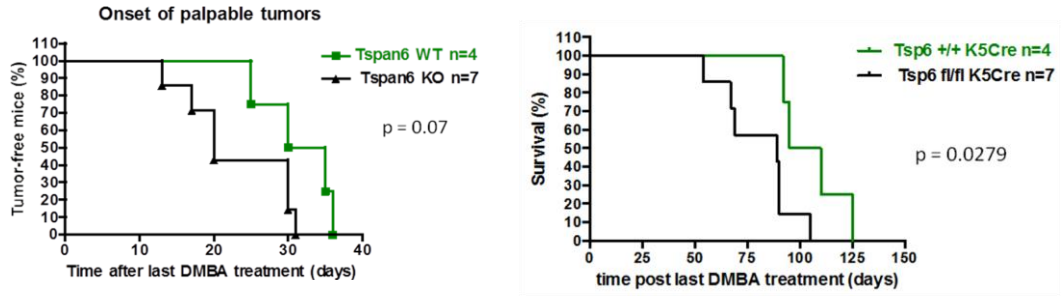

Figure 12. Onset of palpable mammary tumors (left panel) and overall survival (right panel) in K5-Cre TSPAN6fl/fl and TSPAN6 expressing control littermates treated with the progestin MPA and the carcinogen DMBA. Data are shown as percentage of tumor free mice after the last DMBA challenge.

3. Development of haploid ES cell technologies.

Background: Genetic screens have markedly contributed to the understanding of basic physiology and disease pathways[29]. A drawback of genetic screens in cell culture is that one needs to derive cells from homozygously mutated animals or target a gene twice since mammalian cell culture systems are unable to undergo sexual reproduction cycles[29]. RNA-mediated gene knock-down can partially overcome the limitation to study gene function[30]. While having led to multiple breakthroughs, RNA-based gene dowregulation suffers from sometimes inefficient and transient knock-down or off target effects[31,32]. Furthermore, the magnitude of the gene knock-down by RNAi or shRNA varies within cell populations and cells with inefficient knock-down of genes promoting proliferation or survival exhibit a growth advantage, especially in *in vivo* models[33].

Results: My group was among the first in the world to develop haploid ES cells, i.e. stem cells with a single set of chromosomes[34]. We now spent considerable efforts to develop very efficient gene trap vectors for genome-wide mutagenesis that are conditional and can be reverted to wild type via Cre-recombinase as well as back to a null allele via Flippase thereby allowing immediate confirmation of the candidate gene[35] (Figure 13, left panel). After mutagenesis at the haploid stage, these cells duplicate the genome within 1-2 weeks to become diploid, i.e. we can evaluate the effects of mutations in a close to normal genetic setting. Moreover, each clone carries its own genetic barcode to be able to perform quantitative genome-wide screens. Since each system has defined hotspots of integration, we cloned and established multiple insertional mutagenesis vectors, based on retrovirus and lentivirus backbones as well as *Sleeping Beauty* and *Tol2* transposon (Figure 13, right panel). Importantly, when we combine all the mutagenesis system our data indicate that we have been able to develop systems for near-genome saturated mutagenesis. Moreover, we generated intragenic footprints of mutagenesis for each mutagenesis system (Figure 13b).

Of note we now routinely generate between 50-700 Million integrations in a single experiment using about 1 billion sorted haploid ES cells as the starting point. Importantly, when combined we nearly hit every protein coding gene in the genome. Thus, we have been able to successfully set up a system that makes it possible to perform genome-wide, unbiased insertional mutagenesis. The resulting clones carry insertions that can be repaired and carry a barcode. The surviving cells can be selected, for instance selected for synthetic lethality testing cancer drugs on sensitized background (backgrounds we can either engineer or develop from mutant mouse strains such as BRCA1/p53 mutant mice), and the integrations mapped using 4D Sudoku sequencing. Thus, within a short time-period it is now possible to identify essential pathways implicated in e.g. the survival of our cells in response to cytotoxic cancer drugs.

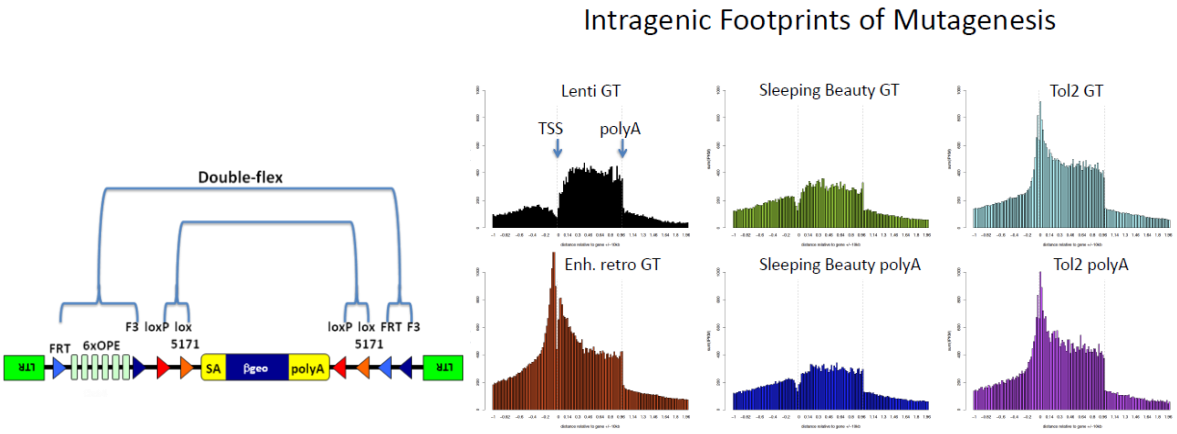

Figure 13. Left panel: Schematic representation of mutagenesis vectors we developed. The double flex (twice revertable) system is indicated in the left panel. Right panels show the insertional mutagenesis vectors we have developed in the last year based on retro and lentiviral LTRs (long terminal repeats), and two different Transposons (Sleeping beauty = SB; and Tol2). OPE sites allow integration into coding genes not expressed in ES cells[32]. SA, splice/acceptor sites. BC, unique genetic barcode added to each clone. Right panels: Intragenic footprints using the indicated mutagenesis vectors. The color scheme indicates numbers of integrations in genes based on reads. TSS, transcriptional start site. GT refers to an exon trap vector; polyA refers to a poly-trap vector. Enh, retro = enhanced retroviral system.

Importantly, using our murine haploid embryonic stem cells und the above described mutagenesis system, we have initiated a cell bank, called Haplobank, in order to develop a library of ES cell clones where nearly every expressed gene carries a homozygous, repairable and bar-coded loss of function mutation. We initially proposed to derive, isolate, expand, freeze and map ~ 50.000 independent mutant clones as an initial step towards the goal of a genome wide collection of null alleles, not knowing about the frequencies of insertional mutagenesis, insertional hotspots etc. We have now picked and mapped 46882 individual ES cell clones, 35589 of which carry a single integration. 20602 of these integrations are intragenic and should disrupt gene expression based on the set-up of our trap vectors. This however needs to be tested for each clone. Our insertions are associated with 23949 different genes (nearly the entire expressed mouse genome), of which 12449 different protein-coding genes carry intragenic insertions. 8159 ES cell clones with intragenic integrations in protein coding genes carry a single integration (Figure 14).

Thus, we have set-up mutagenesis systems with various vector systems that will allow us to perform near-genome saturated forward genetics and we have generated ES cell clones that now can be used for reverse genetics and will be made available to all researchers. We have also started to clone a CRIPR-Cas9 based library to combine this system of genome engineering with the power of haploid genetics.

	Mapped Clones	Multiple Insertions	Single Insertions	Intragenic
Tol2	14259	6875	7384 (52%)	4961(67%)
Lenti	13463	1407	12056 (90%)	8043 (67%)
Retro	19160	3011	16149 (84%)	7598 (47%)
∑	**46 882**	10631	35589 (76%)	**20602 (58%)**

Number of genes associated to insertions	
All associated genes	23949
Genes with intragenic insertions	**11 449**
In clones with single insertion mapped	**8 159**
Tol2	3757
Lenti	4332
Retro	3746

Figure 14. Numbers of total clones mapped, single and multiple insertions in individual clones and the numbers and frequencies of intragenic insertions. The bottom panel shows total numbers of genes carrying intragenic insertions, clones with mapped single intragenic insertions (8159) and the indicated vectors used to generate such single insertional clones.

RESEARCH ACCOMPLISHMENTS:

- **Continued elucidation of RANKL/RANK activation pathways in mammary cancer development**
- **Generation of mice to assess the role of the RANKL/RANK system in BRCA1-driven mammary cancer**
- **Demonstration that RANK has a key role in BRCA1 mutant mammary cancer**
- **Mechanistic elucidation on RANK-driven mammary tumor pathways in a BRCA1/p53 mutant background**
- **Generation of a systems map for genes that cooperate with Ras in epithelial transformation**
- **Cross-validation of our fly hits with thousands of human tumors**
- **Identification of TSPAN6 as a prognostic biomarker for a subtype of breast cancer**
- **Experimental validation of TSPAN6 as a novel tumor suppressor gene in breast cancer**
- **Development of efficient insertional mutagenesis vectors and set-up of near-genome wide screening system using haploid stem cells**

- **Generation of mutant ES cells clones with intragenic insertions covering ~ half of entire protein coding mouse genome.**

REPORTABLE OUTCOMES:

We are setting up a homepage (**Haplobank)** were we will deposit all our mutant ES cell clones. All insertions are mapped, linked to genome browsers, protein sites, PubMed, etc. All clones will be provided for cost and will be accessible to the research community. We hope that we become the key site for functional haploid ES cell genetics in the world providing technologies that should allow all cancer researchers in the world to rapidly perform experiments to validate cancer pathways, screen for pathways of toxic drugs, or elucidate synthetic lethals.

CONCLUSION:

We combine fly genetics and near-genome wide mutagenesis using our haploid ES cells with the vision to perform rapid functional characterization of candidate breast cancer genes. The transgenic RNAi library is covering the whole *Drosophila* genome, giving us an opportunity to examine the function of human candidate cancer genes. Using fly genetics, we have already discovered and experimentally validated a novel tumor suppressor gene, the surface receptor TSPAN6, in mammary cancer development. TSPAN6 expression also correlates with the prognosis of breast cancer in humans, providing a possible novel biomarker to stratify breast cancer risk. Moreover, we have started to generate a haploid murine ES cell library. The haploid ES cell library will be made available to all other breast cancer researchers and could markedly drive the field in the future because any new candidate gene/pathway could be immediately tested *in vivo*.

We have previously identified RANKL/RANK as a key "missing link" between sex hormones and the initiation of mammary cancer. We have now expanded this finding to cancer driven by BRCA1 mutations. Our results in mouse models indicate that genetic ablation of RANK markedly delays and in some cases even abolishes the development of BRCA1/p53 mutation-driven mammary cancer. Thus, if these data can be translated to humans, and considering that an anti-RANKL blocking antibody has already been approved for human use, our data provide a rationale for clinical trials to possibly prevent and delay the development of triple negative breast cancer.

REFERENCES:

1. Kong, Y.-Y., Yoshida, H., Sarosi, I., Tan, H.-L., Timms, E., Capparelli, C., Morony, S., Van, G., Dunstan, C. R., Lacy, D. L., Timms, E., Mak, T. W., Boyle, W. J., and **Penninger, J. M**. OPG-L is a key regulator of osteoclast differentiation, T cell activation, and lymph node organogenesis (Article). **Nature** 397, 315-323. 1999.

2. Kong, Y.-Y., Feige, U., Sarosi, I., Bolon, B., Tifuri, A., Elliott, R., McCabe, S., Casey, J., Wong, T., Campagnuolo, G., Moran, E., Bogoch, E., Cheng, Y., Julian, E., Nguyen, L. T., Ohashi, P. S., Lacey, D. L., Fish, E., Boyle, W. J. and Penninger, J. M. Activated T cells regulate bone loss and joint destruction in arthritis via OPGL. **Nature** 402, 304-309. 1999.

3. Fata, J. E., Kong , Y.-Y., Ji Li, Moorehead, R. A., Elliott, R., Scully, S., Sasaki, T., Ilie-Sasaki, J., Lacey, D. L., Boyle, W. J., Khokha, R., and Penninger, J. M. The osteoclast differentiation factor Osteoprotegerin-Ligand is essential for mammary gland development. **Cell** 103, 41-50. 2000.

4. Jones, H. D., Nakashima, T., Sanchez, O., Kozieradzki, I., Komarova, S. V, Sarosi, I., Morony, S., Rubin, E., Sarao, R., Hojilla, C. V., Komnenovic, V., Kong, Y.-Y., Schreiber, M., Dixon, F. J., Sims, S. M., Khokha, R., Wada, T., and Penninger, J. M. Chemotactic regulation of cancer cell migration and bone metastasis by RANKL. **Nature** 440, 692-496. 2006.

5. Gonzalez-Suarez, E., Jacob, A.P., Jones, J., Miller, R., Roudier-Meyer, M.P., Erwert, R., Pinkas, J., Branstetter, D., and W. C. Dougall. RANK ligand mediates progestin-induced mammary epithelial proliferation and carcinogenesis. **Nature.** 468, 103-107. 2010.

6. Tan, W., Zhang, W., Strasner, A., Grivennikov, S., Cheng, J.Q., Hoffman, R.M., and M. Karin. Tumour-infiltrating regulatory T cells stimulate mammary cancer metastasis through RANKL-RANK signalling. **Nature.** 470, 548-553. 2011.

7. Smith M.R., Saad F., Coleman R., Shore N., Fizazi K., Tombal B. *et al.*. Denosumab and bone-metastasis-free survival in men with castration-resistant prostate cancer: results of a phase 3, randomised, placebo-controlled trial. **Lancet** 379, 39-46. 2012.

8. Canon, J.R., Roudier, M., Bryant, R., Morony, S., Stolina, M., Kostenuik, P.J., Dougall, W.C. Inhibition of RANKL blocks skeletal tumor progression and improves survival in a mouse model of breast cancer bone metastasis. **Clin. Exp. Metastasis.** 25, 119-129. 2008.

9. Rossouw, J.E. et al. Risks and benefits of estrogen plus progestin in healthy postmenopausal women: principal results From the Women's Health Initiative randomized controlled trial. *JAMA* **288**, 321-33 (2002).

10. Beral, V. Breast cancer and hormone-replacement therapy in the Million Women Study. *Lancet* **362**, 419-27 (2003).

11. Cummings SR, San Martin J, McClung MR, Siris ES, Eastell R, Reid IR, Delmas P, Zoog HB, Austin M, Wang A, Kutilek S, Adami S, Zanchetta J, Libanati C, Siddhanti S, Christiansen C; FREEDOM Trial. Denosumab for prevention of fractures in postmenopausal women with osteoporosis. **N Engl J Med.** 361, 756-765. 2009.

12. Smith MR, Egerdie B, Hernández Toriz N, Feldman R, Tammela TL, Saad F, Heracek J, Szwedowski M, Ke C, Kupic A, Leder BZ, Goessl C; Denosumab HALT Prostate Cancer Study Group. Denosumab in men receiving androgen-deprivation therapy for prostate cancer. **N Engl J Med.** 361, 745-755. 2009.

13. Beleut, M., Rajaram, R.D., Caikovski, M., Ayyanan, A., Germano, D., Choi, Y., Schneider, P., Brisken, C. Two distinct mechanisms underlie progesterone-induced proliferation in the mammary gland. **Proc Natl Acad Sci U S A.** 107, 2989-2994. 2010.

14. Schramek, D., Leibbrandt, A., Sigl, V., Kenner, L., Pospisilik, J. A., Lee, H., Hanada, R., Joshi, P. A., Aliprantis, A., Glimcher, L., Pasparakis, M., Khokha, R., Ormandy, C. J., Widschwendter, M., Schett, G., and J. M. Penninger. Osteoclast differentiation factor RANKL controls development of progestin-driven mammary cancer. **Nature,** 468, 98-102. 2010.

15. Nakashima, T., Hayashi, M., Fukunaga, T., Kurata, K., Oh-Hora, M., Feng, J.Q., Bonewald, L.F., Kodama, T., Wutz, A., Wagner, E.F., Penninger, J.M., and H. Takanayagi. Evidence for osteocyte regulation of bone homeostasis through RANKL expression. **Nat Med.** 17, 1231-1234. 2011.

16. Poole AJ, Li Y, Kim Y, Lin SC, Lee WH, Lee EY. Prevention of Brca1-mediated mammary tumorigenesis in mice by a progesterone antagonist. **Scienc**e. 314, 1467-7140. 2006.

17. Caldeira, J., Pereira, P.S., Suriano, G., and Casares, F. Using fruitflies to help understand the molecular mechanisms of human hereditary diffuse gastric cancer. **Int. J. Dev. Biol.** 53, 1557-1561. 2009.

18. Reddy, B.V., and Irvine, K.D. (2008). The Fat and Warts signaling pathways: new insights into their regulation, mechanism and conservation. **Development** 135, 2827-2838. 2008.

19. Vaccari, T., and Bilder, D. At the crossroads of polarity, proliferation and apoptosis: the use of Drosophila to unravel the multifaceted role of endocytosis in tumor suppression. **Mol. Oncol.** 3, 354-365. 2009.

20. Artavanis-Tsakonas, S., Matsuno, K., and Fortini, M.E. Notch signaling. **Science** 268, 225-232. 1995.

21. Brumby, A.M., and Richardson, H.E. scribble mutants cooperate with oncogenic Ras or Notch to cause neoplastic overgrowth in Drosophila. **EMBO J.** *22*, 5769-5779. 2003.

22. Pagliarini, R.A., and Xu, T. A genetic screen in Drosophila for metastatic behavior. **Science** 302, 1227-1231. 2003.

23. http://stockcenter.vdrc.at/control/main

24. Chen, J., Lui, W.O., Vos, M.D., Clark, G.J., Takahashi, M., Schoumans, J., Khoo, S.K., Petillo, D., Lavery, T., Sugimura, J., *et al.* The t(1;3) breakpoint-spanning genes LSAMP and NORE1 are involved in clear cell renal cell carcinomas. **Cancer Cell** 4, 405-413. 2003.

25. Perou, C.M., Sorlie, T., Eisen, M.B., van de Rijn, M., Jeffrey, S.S., Rees, C.A., Pollack, J.R., Ross, D.T., Johnsen, H., Akslen, L.A., et al. Molecular portraits of human breast tumours. **Nature** 406, 747-752. 2000.

26. Loi, S., Haibe-Kains, B., Desmedt, C., Lallemand, F., Tutt, A.M., Gillet, C., Ellis, P., Harris, A., Bergh, J., Foekens, J.A., *et al.* (2007). Definition of clinically distinct molecular subtypes in estrogen receptor-positive breast carcinomas through genomic grade. **J Clin Oncol** *25*, 1239-1246. 2007.

27. Zhang, Y., Sieuwerts, A.M., McGreevy, M., Casey, G., Cufer, T., Paradiso, A., Harbeck, N., Span, P.N., Hicks, D.G., Crowe, J., *et al.* (2009). The 76-gene signature defines high-risk patients that benefit from adjuvant tamoxifen therapy. **Breast Cancer Res Treat**. *116*, 303-309. 2009.

28. Ma, X.J., Wang, Z., Ryan, P.D., Isakoff, S.J., Barmettler, A., Fuller, A., Muir, B., Mohapatra, G., Salunga, R., Tuggle, J.T., *et al.*. A two-gene expression ratio predicts clinical outcome in breast cancer patients treated with tamoxifen. **Cancer Cell** *5*, 607-616. 2004.

29. Nüsslein-Volhard, C., and Wieschaus, E. Mutations affecting segment number and polarity in Drosophila. **Nature** 287, 795-801. 1980.

30. Elbashir et al., 2001 S.M. Elbashir, J. Harborth, W. Lendeckel, A. Yalcin, K. Weber and T. Tuschl, Duplexes of 21-nucleotide RNAs mediate RNA interference in cultured mammalian cells. **Nature** 411**,** 494–449. 2001.

31. Brummelkamp, T.R., Bernards, R., Agami, R. A system for stable expression of short interfering RNAs in mammalian cells. **Science** 296, 550-503. 2002.

32. Bassik, M.C., R.J. Lebbink, L.S. Churchman, N.T. Ingolia, W. Patena, E.M. LeProust, M. Schuldiner, J.S. Weissman and M.T. McManus. Rapid creation and quantitative monitoring of high coverage shRNA libraries. ***Nat. Methods*** 6**,** 443-455. 2009.

33. Fellmann, C., Zuber, J., McJunkin, J., Chang, K., Malone, C.D., Dickins, R.A., Xu, Q., Hengartner, M.O., Elledge, S.J., Hannon**,** G.J., and S. W. Lowe. Functional Identification of Optimized RNAi Triggers Using a Massively Parallel Sensor Assay. **Mol Cell.** 41, 733-746. 2011.

34. Elling, U., Taubenschmid, J., Wirnsberger, G., O'Malley, R., Demers, S.P., Vanhaelen, Q., Shukalyuk, A.I., Schmauss, G., Schramek, D., Schnuetgen, F., von Melchner, H., Ecker, J.R., Stanford, W.L., Zuber, J., Stark, A., and J.M. Penninger. Forward and reverse genetics through derivation of haploid mouse embryonic stem cells. **Cell Stem Cell**. 9, 563-74. 2011.

35. Schnütgen, F., Hansen, J., De-Zolt, S., Horn, C., Lutz, M., Floss, T., Wurst, W., Noppinger, P.R., von Melchner, H. Enhanced gene trapping in mouse embryonic stem cells. **Nucleic Acids Res.** 36, e133. 2008.

APPENDICES:

MPA/DMBA-induced mammary carcinogenesis. MPA/DMBA treatment was performed as described[14]. Briefly, six-week old female mice were anesthetized with ketamine-xylazine and surgically implanted with slow-release Medroxyprogesterone Acetat (MPA) pellets (50mg, 90-day release; Innovative Research of America) subcutaneously on the right flank. 200µl DMBA (5mg/ml diluted in cottonseed oil) was administered by oral gavage 6 times throughout the following 8 weeks. Onset of mammary tumors was determined by palpation.

Statistics. For the Kaplan-Meier analysis of tumor onset a log rank test was performed. $P < 0.05$ was accepted as statistically significant.

SUPPORTING DATA:

All relevant data are shown in the main description of the tasks.